Noise-induced synchronization in small world networks of phase oscillators

Reihaneh Kouhi Esfahani, Farhad Shahbazi,* and Keivan Aghababaei Samani
Department of Physics, Isfahan University of Technology, Isfahan 84156-83111, Iran
(Received 20 November 2011; published 6 September 2012)

A small-world (SW) network of similar phase oscillators, interacting according to the Kuramoto model, is studied numerically. It is shown that deterministic Kuramoto dynamics on SW networks has various stable stationary states. This can be attributed to the so-called *defect patterns* in an SW network, which it inherits from deformation of *helical patterns* in its regular parent. Turning on an uncorrelated random force causes vanishing of the defect patterns, hence increasing the synchronization among oscillators for moderate noise intensities. This phenomenon, called *stochastic synchronization*, is generally observed in some natural networks such as the brain neural network.

DOI: 10.1103/PhysRevE.86.036204 PACS number(s): 05.45.Xt, 87.19.lc, 89.75.Hc

I. INTRODUCTION

Noise is usually considered a source of disturbance for the main signals in the laboratory as well as in natural systems. Nevertheless, the interplay between randomness, created by the noise, and nonlinearities may lead to the enhancement of regular behavior in some dynamical systems [1]. Stochastic resonance [2], coherence resonance [3], noise-induced transport [4], noise-induced transition [5], and noise-induced collective firing in excitable media [6] are examples of such a novel phenomenon. Being noisy, nature takes advantage of these mechanisms to employ random fluctuation as an agent of self-organization. This is the main reason why living systems work so reliably in spite of the presence of various sources of noise.

Brain neurons are examples of biological systems in which the source of random fluctuations is the background synaptic noises caused by highly fluctuating inputs coming from thousands of other neurons connected to a given neuron [7]. However, this noise plays a constructive role in the regular spiking of the individual neurons and also in increasing synchronization among clusters of connecting neurons [8]. Synchronous spiking among a subset of neurons plays an important role in more efficient propagation of activities from one group of neurons to another [9]. Furthermore, there are some controversial ideas on encoding of information about stimuli thorough synchrony in oscillatory activity of neurons [10]. Another phenomenon in which noise-induced synchronization takes place is the gene regulatory process in systems such as quorum-sensing bacteria, in which noise originates from the small number of molecules involved in related biochemical reactions [11].

Collective dynamical behaviors, like synchronization, can be observed in systems of coupled nonlinear oscillators and have been extensively studied in complex networks [12]. One such model has been proposed by Kuramoto, which consists of a set of oscillators of a fixed amplitude (phase oscillators) mutually coupled by a 2π periodic interaction [13]. The stochastic Kuramoto model has been studied on globally connected [14] and also on scale-free (SF) and Erdös-Rènyi (ER) random networks [15]. Analytical results on an all-to-all network show that for a given distribution of intrinsic frequencies of oscillators, a minimum value of coupling is needed for synchronization. Perturbation of the fully synchronized state by uncorrelated white noise causes the synchrony between oscillators to decrease monotonically upon an increase in the noise strength. The same results have been found in numerical integrations of the stochastic Kuramoto model for ER and SF networks.The difference is that the synchronized state in SF networks persists better against application of noise with respect to ER and all-to-all networks [15].

Watts and Strogatz (WS) found out that many systems in nature possess the properties of small-world (SW) networks [16,17]. A short mean path between the nodes and a high degree of clustering are the two main features of SW networks. The former is a characteristic of random networks, while the latter is a feature of regular networks. It has been found that the presence of random shortcuts may lead to noise-driven ordering phenomena such as stochastic resonance [18] and coherence resonance [19] in SW networks.

Motivated by recent discoveries revealing the SW topology of brain neural networks [20] and also noise-induced regulatory behaviors in such networks [8], we study the effect of random force on the dynamics of an SW network of a set of similar phase oscillators coupled to each other based on the Kuramoto model. We show that in this system, for an intermediate noise strength, the synchronization among the oscillators is increased. The rest of the paper is organized as follows. In Sec. II we present the results of numerical integration of the deterministic Kuromato model in regular and SW networks. Investigation of the stochastic Kuramoto model driven by uncorrelated white noise is done in Sec. III, and the final section is devoted to a summary and concluding remarks.

II. KURAMOTO MODEL ON COMPLEX NETWORKS

In this section we introduce the Kuramoto model and numerically investigate its steady-state solutions in ER, SF, and SW networks. Consider a set of phase oscillators, residing on top of the nodes of a network. Their phases and intrinsic oscillation frequencies are given by θ_i and ω_i, respectively. According to the Kuramoto model, the dynamics of these phase oscillators is given by the following set of coupled differential

*shahbazi@cc.iut.ac.ir

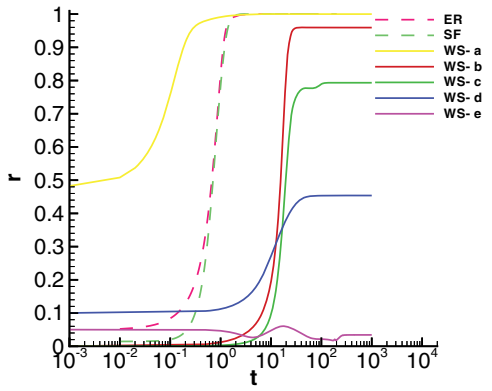

FIG. 1. (Color online) Order parameter (r) versus time (on a logarithmic scale) for ER [dark-gray (fuchsia) dashed curve], Barabási-Albert [light-gray (green) dashed curve], and WS networks for five initial conditions (solid curves for, from top to bottom, WS-a to WS-e). $N = 1000$ and $\langle k \rangle = 10$.

equations:

$$\dot{\theta}_i = \omega_i + K \sum_{j=1}^{N} a_{ij} \sin(\theta_j - \theta_i), \quad i = 1, \ldots, N, \qquad (1)$$

where K is the coupling strength, N is the number of nodes, and a_{ij} are the elements of the adjacency matrix ($a_{ij} = 1$ if nodes i and j are connected and $a_{ij} = 0$ otherwise).

Synchronization of the Kuramoto model for SW networks, for a random distribution of ω_i, has already been studied by Hong *et al.* [21]. They showed that a small fraction of shortcutsis enough for both phase and frequency synchronization, despite the absence of any synchronization of regular ones. In the present work, we assume that all the intrinsic frequencies are the same ($\omega_i = \omega_0$), therefore moving to a reference frame

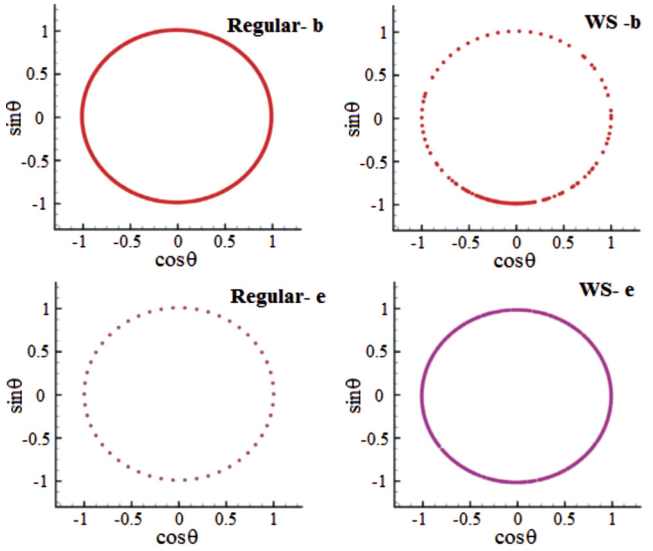

FIG. 2. (Color online) Steady-state phase configurations in two helical patterns of a regular network and corresponding steady states of WS networks with $N = 1000$ and $\langle k \rangle = 10$. WS-b, $\lambda = 1000$; WS-e, $\lambda = 50$. λ is the wavelength of helical states in the regular network.

in which $\omega_0 = 0$ simplifies Eq. (1) to

$$\dot{\theta}_i = K \sum_{j=1}^{N} a_{ij} \sin(\theta_j - \theta_i), \; i = 1, \ldots, N. \qquad (2)$$

To compare the solutions of Kuramoto model in these three networks, we need to construct them with equal numbers of nodes and edges. To build an SF network with average connectivity $\langle k \rangle = 2m$, we use the Barabási-Albert algorithm [22]. Starting from m_0 initial connected nodes, one attaches a newly entering node to $m \leqslant m_0$ older ones with a probability proportional to the degree of the present nodes. An ER random network with N nodes and the same average degree per node ($\langle k \rangle = 2m$) is simply produced by connecting a randomly chosen pair of nodes with Nm edges [23]. To construct the SW network, we use the WS algorithm [16]. Starting from a regular network with N nodes and $k = 2m$ edges for each

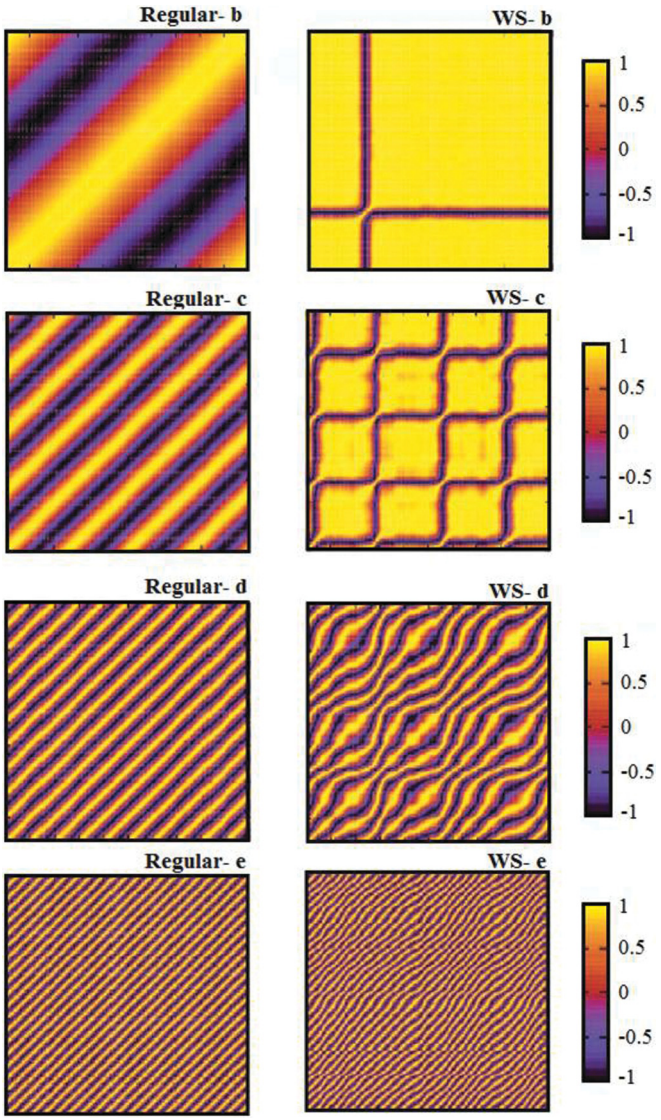

FIG. 3. (Color online) Density plot of correlation matrix elements (D_{ij}) for four helical states of a regular network and corresponding stationary states in a WS network with $N = 1000$ and $\langle k \rangle = 10$. (b) $\lambda = 1000$, (c) $\lambda = 250$, (d) $\lambda = 100$, and (e) $\lambda = 50$. λ is the wavelength of helical states in the regular network.

node, we rewire each edge randomly with probability p. Choosing $0.005 \lesssim p \lesssim 0.05$, this process converts the initial regular network to a complex network with a small mean path length and a large clustering coefficient, characteristics of SW networks.

Starting from a randomly distributed initial phase $\theta_i(0)$ (which is selected from a box distribution in the interval $[-\pi,\pi]$), the set of coupled differential equations, (2), is integrated from $t = 0$ to a given time t with the time step dt, using the Euler method. This method enables us to compute$\theta_i(t)$, and to determine the synchrony among the oscillators at any time we define the complex order parameter

$$re^{i\psi} = \frac{1}{N}\sum_{j=1}^{N} e^{i\theta_j(t)}, \tag{3}$$

where $0 \leqslant r(t) \leqslant 1$ indicates the degree of synchronization in the network and ψ is the phase of the order parameter.

Figure 1 shows the temporal variations of $r(t)$ in the three types of networks with $N = 1000$ and $\langle k\rangle = 10$. To obtain these plots, the time step is set to $dt = 0.01$ and five realizations of the initial phase distribution are taken for a fixed network of each type. The rewiring probability for constructing a WS network from a regular one is chosen to be $p = 0.04$. As shown, the oscillators on ER and Barabási-Albert networks immediately reach a fully synchronized state ($r = 1$) irrespective of the initial conditions. However, in the case of a WS network, they go more slowly toward the steady states, which are highly dependent on the initial phase distributions in such a way that $r(\infty)$ reaches several values between 0 and 1. These results show that, in contrast to ER and SF networks, the structure of steady states of the Kuramoto model of SW networks can be more complex. In what follows, we discuss that the sensibility of dynamics to initial conditions is indeed inherited by SW networks from their regular-network parents. In a regular network, the ratio of nearest neighbor connections to network size (k/N) determines the number of stable solutions. It has been shown that for $k/N < 0.34$, different initial conditions lead to different final states [24].

It is easy to show that the stable stationary solutions of Eqs. (2) have to satisfy the conditions

$$\sum_{i=1}^{N}\sin\theta_i = \sum_{i=1}^{N}\cos\theta_i = 0, \tag{4}$$

provided that the phase difference between any two adjacent oscillators is less than $\pi/2$ (i.e, $\Delta\theta_{ij} = \theta_i - \theta_j < \pi/2$ if $a_{ij} = 1$). These solutions can be put into two categories: (i) fully synchronized states with $r = 1$ ($\Delta\theta_{ij} = 0$ for any i,j) and (ii) phase-locked states with a regular arrangement of phases around the phase circle with nonzero phase difference $\Delta\theta$, for which $r = 0$.

The phase-locked states represent helical-wave phase modulations and their number depends on N and k. For instance, in the case of $N = 1000$ and $k = 10$, there are 10 such states with nearest neighbor phase differences $\Delta\theta^{\alpha}_{nn} = 2\pi/\lambda^{\alpha}$, in which $\lambda^{\alpha} = 20, 25, 40, 50, 100, 125, 200, 250, 500, 1000$ are the wavelengths of the helical states indicated by $\alpha = 1, 2, \ldots, 10$, respectively.

The stationary phase configuration of all nodes, corresponding to the initial conditions in Fig. 1, are plotted in Fig. 2 for both the regular network and its offspring WS network. This plot corresponds to helical patterns with phase differences $\lambda = 1000$ and 50, denoted in Fig. 1 by indexes b and e, respectively. Figure 2 shows that rewiring a regular network with a phase-locked state deforms its helical pattern to an inhomogeneous state in the subsequent WS one. Therefore, a WS network possesses various stable stationary states whose number equals the number of helical patterns in the parent regular network.

The local structure of the steady state can be better clarified by the correlation matrix D, defined as [25]:

$$D_{ij} = \lim_{\Delta t\to\infty}\frac{1}{\Delta t}\int_{t_r}^{t_r+\Delta t}\cos(\theta_i(t) - \theta_j(t))dt, \tag{5}$$

where t_r is the time needed to reach a stationary state. The matrix element $-1 \leqslant D_{ij} \leqslant 1$ is a measure of coherency between each pair of nodes. In the case of full synchrony between i and j ($\theta_i = \theta_j$) the correlation matrix element is $D_{ij} = 1$, and

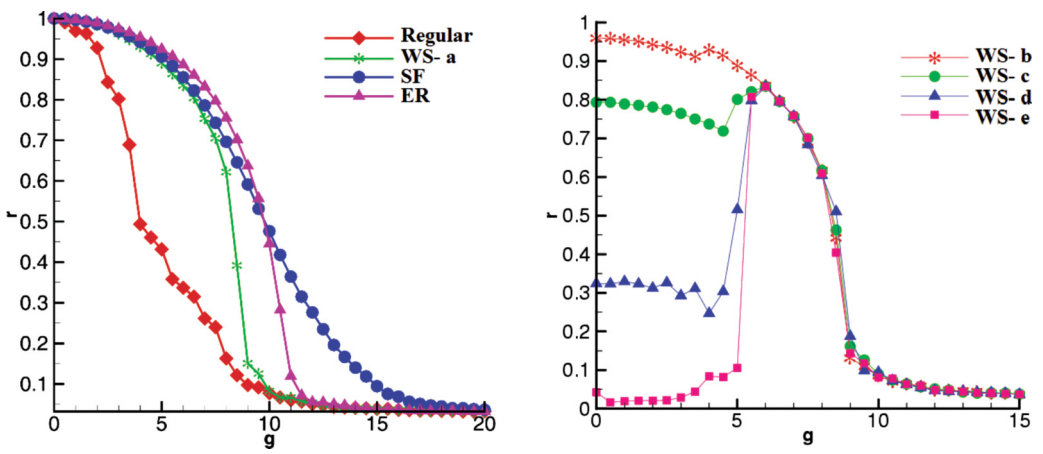

FIG. 4. (Color online) Stationary order parameter versus reduced noise intensity for the four network types. Left: Regular, ER, SF, and fully synchronized states of WS. Right: Four phase-locked states of WS corresponding to states represented in Fig. 3. The number of nodes and mean degree for the three networks are $N = 1000$ and $\langle k\rangle = 10$.

in the case of anti–phase locking ($\theta_i - \theta_j = \pi$), the value of the matrix element is $D_{ij} = -1$. Figure 3 represents a density plot of correlation matrix elements for the four steady states of regular and WS networks corresponding to Figs. 1 and 2. These plots clearly show the inhomogeneous structure of the helical patterns before and after rewiring of the regular network. The correlation matrix represents strip structures in the density plot for helical states in the regular network, and the width of the strips is proportional to the wavelength of the helices. One can also observe from these plots that converting the regular network to a WS one substantially affects the helical patterns, provided that λ is large. The strip structure of matrix D is almost preserved for short wavelengths, indicating that short-wavelength helical patterns, despite small deformations, are stable against rewiring of the network. For long-wavelength patterns of a regular network, the majority of nodes in the corresponding WS phase configurations are synchronized with each other, however, there are some isolated nodes in anti–phase locking from the rest. These isolated nodes are *topological defects* and induce spiral phase textures around them, in such a way that the phase of surrounding oscillators varies continuously from 0 to π, upon getting away from these nodes. The number of these defects increases upon a decrease in the wavelength of the corresponding helical pattern. For example, it can be seen from Fig. 3 that for $\lambda = 1000$ there is one point defect, while for $\lambda = 250$ there are four. Once the structure of the steady states of the deterministic Kuramoto model for a WS network is known, it will be interesting to investigate the effect of noise on such states.

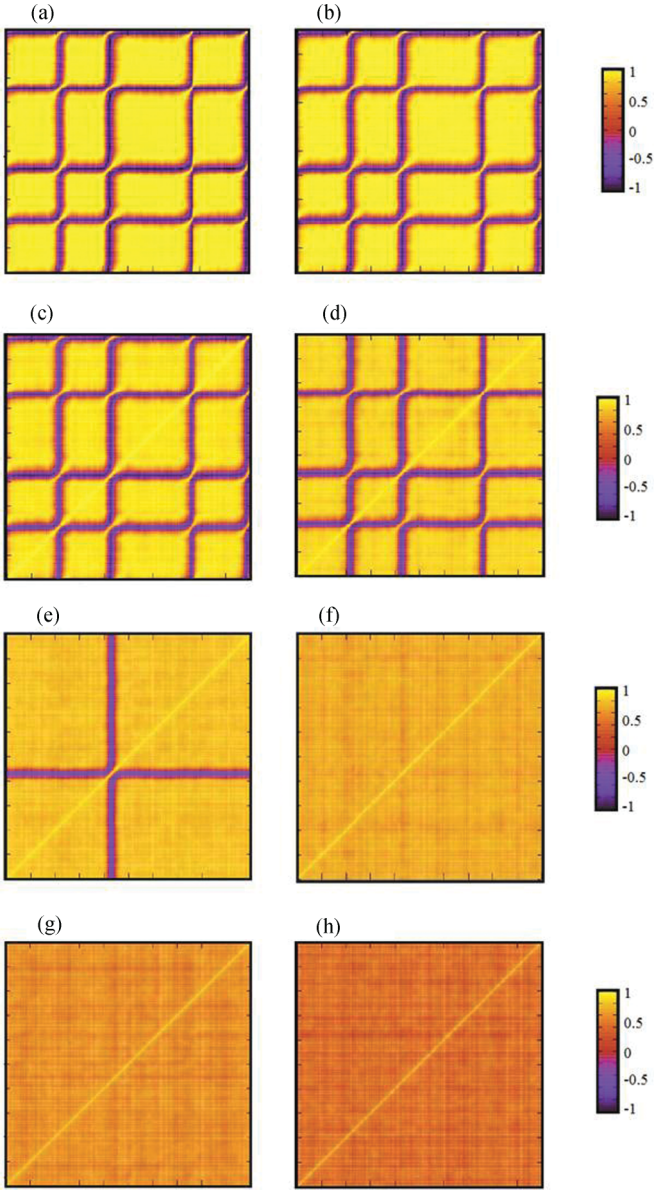

FIG. 5. (Color online) Density plot of correlation matrix elements (D_{ij}) for a steady state with four point defects on an SW network and different noise intensities: (a) $g = 0$, (b) $g = 2$, (c) $g = 3$, (d) $g = 4$, (e) $g = 5$, (f) $g = 6$, (g) $g = 7$, and (h) $g = 8$. The number of nodes and mean degree for the three networks are $N = 1000$ and $\langle k \rangle = 10$.

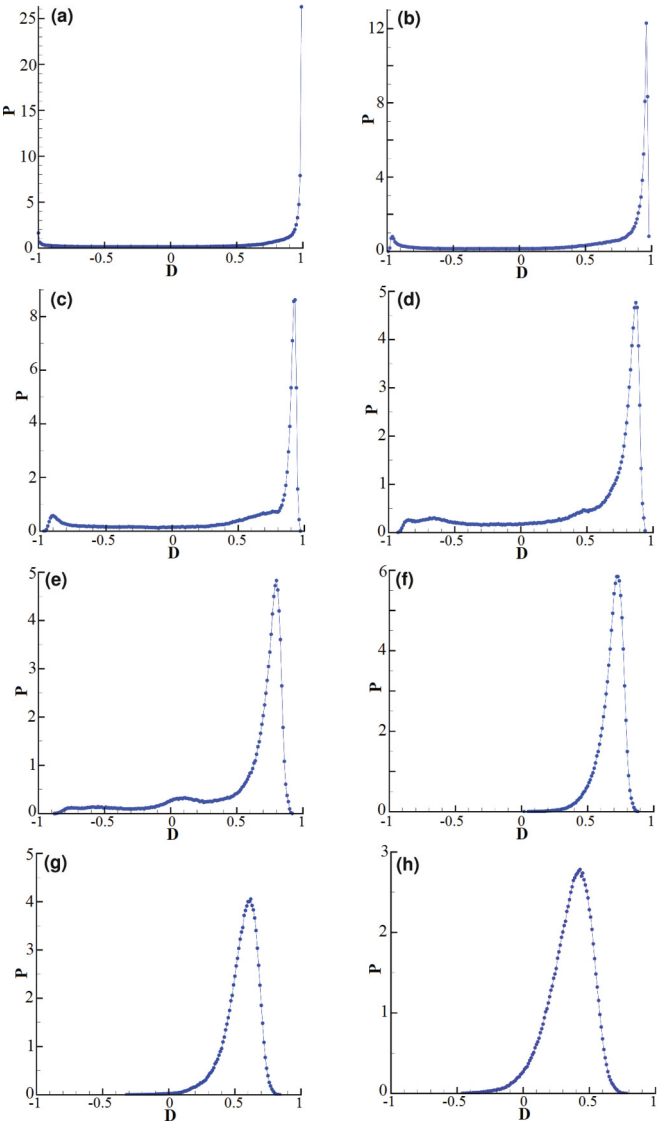

FIG. 6. (Color online) Probability distribution function of correlation matrix elements (D_{ij}) for different noise intensities: (a) $g = 0$, (b) $g = 2$, (c) $g = 3$, (d) $g = 4$, (e) $g = 5$, (f) $g = 6$, (g) $g = 7$, and (h) $g = 8$. The number of nodes and mean degree for the three networks are $N = 1000$ and $\langle k \rangle = 10$.

III. THE EFFECT OF RANDOM FORCE

A network of oscillators could be plagued by some external random forces. The effect of such forces may be modeled by an uncorrelated white noise $[\eta_i(t)]$ applying to all nodes. Adding this noise to Eq. (2), we have

$$\dot{\theta}_i = K\sum_{j=1}^{N} a_{ij}\sin(\theta_j-\theta_i)+\eta_i(t), \quad i=1,\ldots,N, \qquad (6)$$

where $\langle\eta_i(t)\rangle = 0$, $\langle\eta_i(t)\eta_j(t')\rangle = 2D\delta(t-t')\delta_{ij}$, with D being the variance or intensity of the noise. In our numerical work, we choose a box distribution in the interval $[-w/2,w/2]$ for η, so that its variance is equal to $D = w^2/24$. It can be shown that by proper rescaling of the time variable, the effect of parameters D and K can be included in a single parameter $g^2 = \frac{D}{K}$ [15], converting the dynamical equations to

$$\frac{d\theta_i}{d\tau} = \sum_{j=1}^{N} a_{ij}\sin(\theta_j-\theta_i)+g\xi_i(\tau), \qquad (7)$$

where $\tau = Kt$ is the rescaled time variable and $\xi_i(\tau) := \eta_i(t)/g$ is a random variable in the interval $[-1/2,1/2]$.

Numerical integration of Eq. (7) is carried out by employing the Euler method for the deterministic part and Ito's algorithm [26] for the stochastic part. Figure 4 represents the variations of the stationary order parameter $[r(\infty)]$ versus the rescaled noise intensity g for the four network types: regular, SF, ER, and WS (top panel for fully synchronized states and bottom panel for phase-locked ones).

Upon inspecting this figure, one can extract two essential results. (i) As shown in the top panel, for all four networks, the order parameter, starting from a fully synchronized state with $r(\infty) = 1$, decreases monotonically when the noise is turned on. The critical coupling (g_c) at which synchrony among the oscillators disappears is the greatest for the SF and the smallest for the regular network. Therefore the coherent state in the SF network lasts longer against noise than that in the ER, WS, and regular networks with the same average degree and coupling constant. The greater fragility of the fully synchronized state in regular and WS networks can be explained in terms of the formation of some local clusters in these networks. The phase differences among different clusters of oscillators tend to become large due to the effect of random forcing, hence leading to a rapid decrease in the order parameter. The persistence of the synchronized state in the SF network has been argued to be related to the existence of few nodes with a very large number of connections (hubs) in this type of network [15].

(ii) The bottom panel in Fig. 4 shows that for inhomogeneous phase-locked states in the WS network, the variation of $r(\infty)$ versus noise is nonmonotonic. It remains almost constant for small noise strengths and reaches a maximum in an interval of reduced noise intensity. Therefore in these cases, instead of playing a destructive role, noise promotes synchrony among oscillators.

Noise-induced synchronization is also called *stochastic synchronization* and its occurrence in WS networks can be explained in terms of defect patterns in the steady states of the Kuramoto model. Figure 5 represents the evolution of correlation matrix density plots versus a reduced noise intensity, g, for a specific steady state of a WS network with four topological defects. It is shown in this figure thatwhen noise is turned on, the defects resist it up to $g \sim 4$, they begin to disappear at $g > 4$, and they vanish completely at $g \sim 6$. The disappearance of defects enhances the homogeneity in the system and, so, the synchrony among the oscillators. This is more apparent in the probability distribution of correlation matrix elements $[p(D)]$ shown in Fig. 6. As the figure shows, $p(D)$ has two peaks, at $D = 1$ and -1, for $g = 0$. Upon an increase in the noise intensity the two peaks move toward each other, and at the onset of stochastic synchronization, $g \sim 6$, they emerge in one peak. At this point the variance of $p(D)$ reaches its minimum and, again, increases with increasing noise strength. Figure 7 represents the complexity of WS, ER, and SF networks in terms of reduced noise intensity. The complexity is defined by the Shannon entropy of $p(D)$ [27],

$$S = \left(-\sum_{i=1}^{m} p_i \ln p_i\right)/\ln m, \qquad (8)$$

where m is the number of bins in the division of $p(D)$ ($m = 200$ in this work). This quantity measures the ability of a

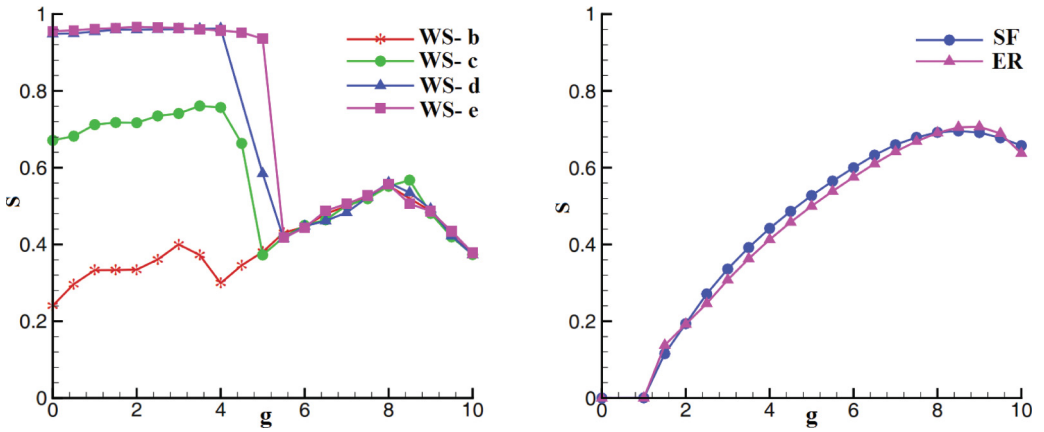

FIG. 7. (Color online) Left: Complexity of small-world network versus noise intensity for $N = 1000$ and $\langle k\rangle = 10$. These plots correspond to initial conditions leading to the helical state in parent regular networks with wavelength $\lambda = 1000$, 250, 100, and 10. Right: Complexity of ER and SF networks versus noise intensity for $N = 1000$ and $\langle k\rangle = 10$.

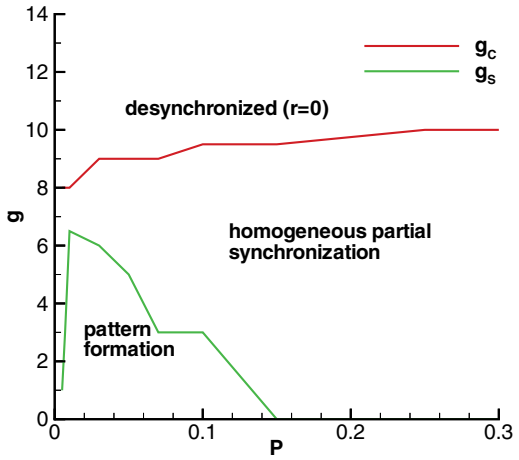

FIG. 8. (Color online) Phase diagram of the noisy Kuramoto model for an SW network with $N = 1000$ and $\langle k \rangle = 10$, in g-p space. g_s [light-gray (green) line] and g_c [dark-gray (red) line] denote the noise strengths at the onsets of stochastic synchronization and desynchronization, respectively.

network both to synchronize as a whole (integration) and, meanwhile, to preserve the independence of its subsystems (segregation). This intermediate regime with a high complexity is desirable for functioning of real neural networks.

In the top panel in Fig. 7, we compare the complexity of the Kuramoto model of a WS network for different initial conditions, leading to the patterns shown in Fig. 3. This plot shows that the complexity is larger for the patterns with greater spatial inhomogeneity (corresponding to the helical patterns with smaller wavelength in the regular networks), and these patterns are more robust against noise. By applying the noise, the complexity remains more or less unchanged until the the onset of stochastic synchronization at which shows a sudden fall. Beyond this point, the complexity tends to rise and reaches to a maximum at the noise strength by which the synchronization vanishes. On the contrary, for ER and SF networks, shown in the bottom panel of Fig. 7, the complexity monotonically raises with noise strength and reaches to a maximum at the onset of the vanishing of synchronization.

Finally, we investigate the occurrence of stochastic synchronization in terms of the link rewiring probability p. We found that the value of the noise strength at which stochastic synchronization occurs reaches a maximum at $p \sim 0.02$ and then decreases with increasing p and vanishes at $p \sim 0.17$. For $p > 0.17$, the behavior of the noisy Kuramoto dynamics in an SW network is similar to that in random networks. Figure 8 depicts the phase diagram for an SW network with $N = 1000$ and $\langle k \rangle = 10$, in g-p space.

IV. CONCLUSION

In summary, we have found that an SW network of similar phase oscillators communicating with each other by Kuramoto coupling shows novel behaviors. Unlike ER and SF networks, this system fails to reach a fully synchronized state for any arbitrary initial conditions. Moreover, driving it with uncorrelated white noise reveals the occurrence of stochastic synchronization, a phenomenon through which a random force induces synchrony among the oscillators. We report that the reason for this phenomenon lies in the stable helical patterns in the regular networks from which the SW networks are built. Rewiring a regular network of similar phase oscillators with a periodic helical pattern results in complex inhomogeneous states in the resulting SW network. The existence of such stable inhomogeneous patterns in SW networks, sometimes appearing as topological point defects and also as aperiodic helical patterns, prevents the network from reaching full synchrony. These patterns persist against the noise at low noise intensities. However, external random forces of moderate strengths are able to destroy these patterns in favor of more homogeneous states, hence enhancing the synchronization among oscillators. We have computed the complexityof the SW network in the case of inhomogeneous pattern formation and shown that the complexity of such states is higher than that of ER and SF networks, for a noise strength less than the onset of stochastic synchronization. Therefore, as a model for neural networks, this finding shows that the functioning of such systems can be more efficient in the presence of moderate noise. Generalization of the above results to the more realistic case in which the coupling constants (coefficients of periodic couplings) are normalized to the degree of the nodes is currently under investigation. We hope that our results will shed light on the reason why SW networks are so ubiquitous in natural systems.

ACKNOWLEDGMENTS

We would like to thanks S. Strogatz for enthusiastic discussion and useful comments.

[1] F. Sagués, J. M. Sancho, and J. García-Ojalvo, Rev. Mod. Phys. **79**, 829 (2007).
[2] L. Gammaitoni, P. Hänggi, P. Jung, and F. Marchesoni, Rev. Mod. Phys. **70**, 223 (1998).
[3] B. Lindner, J. García-Ojalvo, A. Neiman, and L. Schimansky-Geier, Phys. Rep. **392**, 321 (2004).
[4] P. Reimann, Phys. Rep. **361**, 57 (2002).
[5] W. Horsthemke and R. Lefever, *Noise-Induced Transitions* (Springer, Berlin, 1984).
[6] S. Kádár, J. Wang, and K. Showalter, Nature (London) **391**, 770 (1998); S. Alonso, I. Sendiña-Nadal, V. Pérez-Muñuzuri, J. M. Sancho, and F. Sagués, Phys. Rev. Lett. **87**, 078302 (2001); S. Tanabe and K. Pakdaman, Biol. Cybern. **85**, 269 (2001); C. J. Tessone, A. Scirè, R. Toral, and P. Colet, Phys. Rev. E **75**, 016203 (2007).
[7] W. H. Calvin and C. F. Stevens, Science **155**, 842 (1967).
[8] G. B. Ermentrout, R. F. Galán, and N. N. Urban, Trends Neurosci. **31**, 428 (2008).

[9] A. N. Burkitt and G. M. Clark, Neural Comput. **11**, 871 (1999); E. Salinas and T. J. Sejnowski, Nat. Rev. Neurosci. **2**, 539 (2001); A. D. Reyes, Nat. Neurosci. **6**, 593 (2003); P. H. Tiesinga and T. J. Sejnowski, Neural Comput. **16**, 251 (2004).

[10] M. Stopfer *et al*., Nature **390**, 70 (1997); A. K. Engel *et al*., Conscious Cogn. **8**, 128 (1999); M. N. Shadlen and J. A. Movshon, Neuron **24**, 67 (1999); J. A. Movshon, *ibid*. **27**, 412 (2000).

[11] M. Springer and J. Paulsson, Nature **439**, 27 (2006); T. Zhou, L. Chen, and K. Aihara, Phys. Rev. Lett. **95**, 178103 (2005).

[12] A. Arenas, A. Diaz-Guilera, J. Kurths, Y. Moreno, and C. Zhou, Phys. Rep. **469**, 93 (2008).

[13] Y. Kuramoto, *Lecture Notes in Physics* (Springer, New York, 1975), Vol. 39, pp. 420–422; *Chemical Oscillations, Waves, and Turbulence* (Springer, Berlin, 1984).

[14] J. A. Acebrón, L. L. Bonilla, C. J. Pérez Vicente, F. Ritort, and R. Spigler, Rev. Mod. Phys. **77**, 137 (2005); B. C. Bag, K. G. Petrosyan, and C. K. Hu, Phys. Rev. E **76**, 056210 (2007).

[15] H. Khoshbakht, F. Shahbazi, and K. Aghababaei Samani, J. Stat. Mech. (2008) P10020.

[16] J. D. Watts and S. H. Strogatz, Nature **393**, 440 (1998).

[17] S. H. Strogatz, Nature **410**, 268 (2001).

[18] Z. Gao, B. Hu, and G. Hu, Phys. Rev. E **65**, 016209 (2001); H. Hong, B. J. Kim, and M. Y. Choi, *ibid*. **66**, 011107 (2002); M. Perc and M. Gosak, New J. Phys. **10**, 053008 (2008).

[19] O. Kwon and H.-T. Moon, Phys. Lett. A **298**, 319 (2002); O. Kwon, H.-H. Jo, and H.-T. Moon, Phys. Rev. E **72**, 066121 (2005).

[20] D. S. Bassett and E. Bullmore, Neuroscientist **12**, 512 (2006); E. Bullmore and O. Sporns, Nature Rev. Neurosci. **10**, 186 (2009).

[21] H. Hong, M. Y. Choi, and B. J. Kim, Phys. Rev. E **65**, 026139 (2002).

[22] A. L. Barabási and R. Albert, Science **286**, 509 (1999); A. L. Barabasi, R. Albert, and H. Joeng, Physica A **272**, 173 (1999).

[23] P. Erdös and A. Rényi, Publ. Math. Debrecen **6**, 290 (1959); Publ. Math. Inst. Hung. Acad. Sci **5**, 17 (1960).

[24] D. A. Wiley, S. H. Strogatz, and M. Girvan, Chaos **16**, 015103 (2006).

[25] J. Gómez-Gardeñes, Y. Moreno, and A. Arenas, Phys. Rev. Lett. **98**, 034101 (2007).

[26] C. W. Gardiner, *Handbook of Stochastic Methods for Physics, Chemistry and the Natural Sciences* (Springer-Verlag, Berlin, 1980).

[27] M. Zhao, C. Zhou, Y. Chen, B. Hu, and B-H. Wang, Phys. Rev. E **82**, 046225 (2010).